



Missouri University of Science and Technology
Scholars' Mine

Electrical and Computer Engineering Faculty
Research & Creative Works

Electrical and Computer Engineering

01 Dec 1995

The Effect of Excitation Limits on Voltage Stability

Jyothi Ayyagari

Mariesa Crow

Missouri University of Science and Technology, crow@mst.edu

Follow this and additional works at: https://scholarsmine.mst.edu/ele_comeng_facwork

 Part of the [Electrical and Computer Engineering Commons](#)

Recommended Citation

J. Ayyagari and M. Crow, "The Effect of Excitation Limits on Voltage Stability," *IEEE Transactions on Circuits and Systems I: Fundamental Theory and Applications*, vol. 42, no. 12, pp. 1022-1026, Institute of Electrical and Electronics Engineers (IEEE), Dec 1995.

The definitive version is available at <https://doi.org/10.1109/81.481199>

This Article - Journal is brought to you for free and open access by Scholars' Mine. It has been accepted for inclusion in Electrical and Computer Engineering Faculty Research & Creative Works by an authorized administrator of Scholars' Mine. This work is protected by U. S. Copyright Law. Unauthorized use including reproduction for redistribution requires the permission of the copyright holder. For more information, please contact scholarsmine@mst.edu.

- [7] J. Rubinstein, P. Penfield, and M. A. Horowitz, "Signal delay in RC tree networks," *IEEE Trans. Computer-Aided Design*, vol. CAD-2, pp. 202-211, 1983.
- [8] L. A. Glasser and D. W. Dobberpuhl, *The Design and Analysis of VLSI Circuits*. Reading, MA: Addison-Wesley, 1985.
- [9] J. Vlach, J. A. Barby, A. Vannelli, T. Talkhan, and C. J. Shi, "Group delay as an estimate of delay in logic," *IEEE Trans. Computer-Aided Design*, vol. 10, pp. 949-953, 1991.
- [10] K. D. Boese, A. B. Kahng, B. A. McCoy, and G. Robins, "Fidelity and near-optimality of Elmore-based routing constructions," in *Int. Conf. Computer Design*, 1993, pp. 81-84.
- [11] N. H. E. Weste and K. Eshraghian, *Principles of CMOS VLSI Design*. Reading, MA: Addison-Wesley, 1993.
- [12] M. Shoji, *CMOS Digital Circuit Technology*. Englewood Cliffs, NJ: Prentice-Hall, 1988.
- [13] D. Hill, D. Shugard, J. Fishburn, and K. Keutzer, *Algorithms and Techniques for VLSI Layout Synthesis*. New York: Kluwer, 1989.
- [14] H. B. Bakoglu and J. D. Meindl, "Optimal Interconnection Circuits for VLSI," *IEEE Trans. Electron Devices*, vol. ED-32, pp. 903-909, 1985.
- [15] J. L. Wyatt, "Signal propagation delay in RC models for interconnect," *Circuit Analysis, Simulation and Design*, A. E. Ruehli, Ed. Amsterdam: North-Holland, 1987.
- [16] R. Courant and F. John, *Introduction to Calculus and Analysis*. New York: Springer-Verlag, 1989, vol. 2.
- [17] B. W. Char, K. O. Geddes, G. H. Gonnet, B. L. Leong, M. B. Monagan, and S. M. Watt, *Maple V Library Reference Manual*. New York: Springer-Verlag, 1991.
- [18] G. A. Sai-Halasz, "Performance trends in high-end processors," *Proc. IEEE*, vol. 83, pp. 20-36, 1995.

The Effect of Excitation Limits on Voltage Stability

M. L. Crow and J. Ayyagari

Abstract— Voltage collapse has been commonly associated with insufficient reactive power support. Steady state studies have related reactive power generation limitations to the sudden onset of voltage instability. This paper extends this approach to the dynamic case. The relationship between the dynamic models and steady state behavior is established. The dynamic model is then used to investigate the sudden change in system stability when the maximum excitation limit is reached. Several illustrative examples are analyzed. Corrective actions are proposed which will move the physical system away from the region of instability.

I. INTRODUCTION

A voltage collapse is the process by which the sequence of events accompanying voltage instability leads to a low unacceptable voltage profile in a significant part of the power system [1]. Once associated only with weak systems containing long lines, voltage instability and collapse is becoming increasingly prevalent in tightly interconnected systems due to the increased loading on the network. A voltage collapse scenario has been usually described as a slow decline in voltage levels, with little or no deviation in frequency or angle, until a point wherein the voltage levels plummet rapidly. In this scenario, there is little or no oscillatory behavior in the system. Because of this time frame and the lack of transient behavior associated with a true

voltage collapse, many researchers have felt comfortable with the use of models in which only the slowly varying components associated with the generators are explicitly modeled. For this reason, the effects of the excitation system and the automatic voltage regulators (AVR's) are often simplified and/or neglected.

Increasingly however, the effect of the excitation system on voltage stability has received closer scrutiny [2]–[5]. The effect of excitation system limits on voltage stability was first suggested in [2]. In this analysis it was noted that one of the crucial aspects of modeling which is often overlooked is the effect of the generator current limiters. Specifically, if the effects of the limiters are ignored, the modeled reactive output from the generator will remain too high, giving false results which may potentially cause the system to appear to be more stable than it actually is. This is the case when a generator is modeled as having unlimited reactive power generation capabilities. It has recently been shown that a power system may become immediately unstable when the reactive power limit of a generator is encountered [6]. This study showed that a system may pass immediately into an unstable operating region when the generator reaches its reactive power operating limit. This instantaneous change in stability was attributed to a sudden change in the algebraic manifold of the dynamical system when a reactive power limit was encountered, while the system state remained unchanged. In this scenario, the system state may suddenly reside in an unstable or infeasible operating region. The authors further concluded that this structural change is a plausible cause for voltage collapse. Although the possibility of immediate system instability as a result of encountering an excitation system limit has been well accepted in industrial experience, there exists little model development and analysis to account for this phenomenon.

In this brief, the approach in [6] is extended to the case where there is a structural change in the system dynamics, as opposed to the algebraic manifold. This is the case when the dynamic system model is extended to include the dynamics of the automatic voltage regulator and exciter. In this case, one of the dynamic states associated with the exciter will encounter its limit and the governing dynamic equation will be replaced with an algebraic equation. Thus the dynamic system state space will be effectively reduced, and an additional algebraic constraint will be imposed. In this paper, it is this change in system structure which is shown to be responsible for the immediate change in stability when the maximum excitation limit is encountered.

II. THE POWER SYSTEM MODEL

A typical power system model of m generators with automatic voltage regulators (AVR) in an n bus network where winding resistance and saliency have been neglected is [7]:

$$T'_{d0} \dot{E}'_q = -\frac{x_d}{x'_d} E'_q + \frac{(x_d - x'_d)}{x'_d} V \cos(\theta - \delta) + E_{fd} \quad (1)$$

$$T'_{q0} \dot{E}'_d = -\frac{x_q}{x'_d} E'_d - \frac{(x_q - x'_d)}{x'_d} V \sin(\theta - \delta) \quad (2)$$

$$\dot{\delta} = \omega - \omega_s \quad (3)$$

$$M \dot{\omega} = T_M + \frac{V}{x'_d} (E'_d \cos(\theta - \delta) + E'_q \sin(\theta - \delta)) \quad (4)$$

$$T_E \dot{E}_{fd} = -K_E E_{fd} - S_E (E_{fd}) E_{fd} + V_R \quad (5)$$

$$T_A \dot{V}_R = -V_R + K_A \left(R_F - \frac{K_F}{T_F} E_{fd} + (V_{ref} - V) \right) \quad (6)$$

Manuscript received July 18, 1994; revised July 18, 1995. This work was supported in part by the NSF under Grant ECS-9108914. This paper was recommended by Associate Editor M. Ilic.

The authors are with the Intelligent Systems Center and the Department of Electrical Engineering at the University of Missouri, Rolla, MO 65401 USA.
IEEE Log Number 9416045.

TABLE I
EQUILIBRIA AND EIGENVALUES OF THE UNCONSTRAINED SYSTEM

	Equilibrium	Eigenvalues
A-1	$x_1 = \frac{k_2 k_3}{k_1 k_4} y^{sp}$ $x_2 = \frac{k_3}{k_4} y^{sp}$ $y = 0$	$-k_1$ $-k_4$
A-2	$x_1 = \left[\frac{k_2 k_3 k_7}{k_4 (k_3 k_6 - k_1 k_7) + k_2 k_3 k_6} \right] y^{sp}$ $x_2 = \left[\frac{k_3 (k_1 k_7 - k_3 k_6)}{k_4 (k_3 k_6 - k_1 k_7) + k_2 k_3 k_6} \right] y^{sp}$ $y = \left[\frac{-k_2 k_3 k_4}{k_4 (k_3 k_6 - k_1 k_7) + k_2 k_3 k_6} \right] y^{sp}$	$\frac{1}{2} \left(-(k_1 + k_4 + \frac{k_3 k_4}{k_7}) + \sqrt{(k_1 + k_4 + \frac{k_3 k_4}{k_7})^2 - 4 \left(\frac{k_4 (k_1 k_7 + k_3 k_6) - k_2 k_3 k_6}{k_7} \right)} \right)$ $\frac{1}{2} \left(-(k_1 + k_4 + \frac{k_3 k_4}{k_7}) - \sqrt{(k_1 + k_4 + \frac{k_3 k_4}{k_7})^2 - 4 \left(\frac{k_4 (k_1 k_7 + k_3 k_6) - k_2 k_3 k_6}{k_7} \right)} \right)$

$$V_R^{min} \leq V_R \leq V_R^{max}$$

$$T_F \dot{R}_F = -R_F + \frac{K_F}{T_F} E_{fd} \quad (7)$$

where (1)-(4) represent the dynamics of the generator, and (5)-(7) represent the dynamics of the exciter and AVR. The saturation function $S_E(E_{fd})$ is given by $S_E(E_{fd}) = A_{EX} \exp(B_{EX} E_{fd})$ where A_{EX} and B_{EX} are constants chosen to match the open-circuit magnetization curve at two points, usually E_{fd}^{max} and $0.75 E_{fd}^{max}$. The exciter has several protective devices, one of which is the overexcitation or maximum excitation limiter (MXL). The purpose of the MXL is to protect the generator from overheating due to prolonged field overcurrent. The end effect of the MXL is to limit the field current to prevent damage to the generator. Excitation limits may be of the windup or nonwindup type. In a windup limit, the output of the limiter is constrained as long as the measured output exceeds the specified limit. In a nonwindup limit, the output of the limiter is constrained if the measured output exceeds the specified limit and the derivative of the output is greater than zero. With nonwindup limits, the output comes off the limit as soon as the derivative changes sign [1]. Although not as general as in many industrial applications, one common assumption is to model the excitation limit as a windup limit as this tends to be the "worst case scenario [7]." This limiter is represented by the upper limit constraint imposed on (6).

The powerflow network equations are given by:

$$0 = P_i - V_i \sum_{j=1}^n V_j (g_{ij} \cos \theta_{ij} + b_{ij} \sin \theta_{ij}) \quad (8)$$

$$0 = Q_i - V_i \sum_{j=1}^n V_j (g_{ij} \sin \theta_{ij} - b_{ij} \cos \theta_{ij}) \quad (9)$$

for $i = 1, \dots, n$, $\theta_{ij} = \theta_i - \theta_j$, and P_i and Q_i are the injected powers at each bus. For generator buses, these are the real and reactive power generated. At load buses, these are the real and reactive loading on that bus. The inputs to this system are the AVR reference voltage settings V_{refi} , synchronous speed ω_s , and the constant input torque, T_{Mi} , for each machine $i = 1, \dots, m$, and the active and reactive bus loadings P_{Li} and Q_{Li} , for $i = m + 1, \dots, n$.

III. CHANGE OF STABILITY WHEN STATE LIMITS ARE ENCOUNTERED

In this section, the notion of immediate instability as a result of structural changes will be extended to the case where a maximum excitation limit is encountered. The approach presented in this paper focuses on the excitation/AVR system limits and is therefore different from the treatment found in [6], which focused on reactive power

limits. The two limits are physically related, however. The reactive power output of a generator is governed by the field current; if this input is limited, the reactive power generated is also limited. Although the two limits are physically similar, the effect that the particular limiting constraint has on the system may be different.

To illustrate this, consider the following simple system which is intended to represent the operation of a generator, a voltage regulator, and the constraining powerflow equation

$$\dot{x}_1 = -k_1 x_1 + k_2 x_2 + k_3 y \quad (\text{gen}) \quad (10)$$

$$\dot{x}_2 = -k_4 x_2 + k_5 (y^{sp} - y) \quad (\text{AVR}) \quad (11)$$

$$x_2^{min} \leq x_2 \leq x_2^{max}$$

$$0 = k_6 y x_1 + k_7 y^2 - u \quad (\text{ntwk}) \quad (12)$$

where the input u may be taken as the reactive power loading and y^{sp} is the specified reference setting for the algebraic variable y , analogous to the reference voltage setting of the AVR. Note that (12) is quadratic in y , thus multiple solutions for a given loading u are possible. This is analogous to the multiplicity of solutions possible due to the quadratic nature of the voltage in the powerflow equations. For ease of illustration, the input u will initially be taken as 0, which leads to two unique equilibria which are summarized in Table I. Although the full system model of a generator and exciter/AVR has a greater number of states and is nonlinear, the interaction between states is clearer in this simplified model. The conclusions drawn from this example will be generalized to a larger system in the next section.

It is apparent that for the given loading level u , there exist two equilibria as well as two sets of eigenvalues. For this to be a feasible operating point, at least one of the equilibria must be stable, with both corresponding eigenvalues having negative real parts. Since voltage collapse is a nonoscillatory phenomenon, it may be assumed that the parameters $k_1 - k_7$ are such that the resulting eigenvalues are real, with no imaginary parts. Equilibrium A-1 may be considered to be analogous to the operating point which would arise in an unenergized power system, thus, the feasible operating point under consideration will be assumed to be A-2. Now, suppose that the state x_2 has reached its maximum at a particular loading level. At this point the dynamic equation (11) is replaced by the algebraic equation

$$0 = x_2 - x_2^{max} \quad (13)$$

This change in the structure of the dynamical system now yields two equilibrium points which satisfy (10), (12), and (13). These new equilibria and the corresponding eigenvalues are summarized in Table II.

The change in dynamical system structure has several ramifications. First, note that the equilibria A-2 and B-1 are the same points,

TABLE II
EQUILIBRIA AND EIGENVALUES OF THE CONSTRAINED SYSTEM

	Equilibrium	Eigenvalues
B-1	$x_1 = \frac{k_2 k_7}{k_1 k_7 + k_3 k_6} x_2^{max}$ $x_2 = x_2^{max}$ $y = -\frac{k_2 k_6}{k_1 k_7 + k_3 k_6} x_2^{max}$	$-k_1 - \frac{k_3 k_6}{k_7}$
B-2	$x_1 = \frac{k_2}{k_1} x_2^{max}$ $x_2 = x_2^{max}$ $y = 0$	$-k_1$

since at the exact point where $x_2 = x_2^{max}$, both (11) and (13) must be satisfied, and $x_2^{max} = \left[\frac{-k_6(k_1 k_7 + k_3 k_6)}{k_4(k_1 k_7 + k_3 k_6) + k_2 k_5 k_6} \right] y^{sp}$. The equilibrium point B-1 however has only one eigenvalue instead of two associated with it since x_2 is no longer a state variable in the limited system. Instability may arise in several ways. First, the structural change may elicit an immediate change in the stability of the associated equilibrium. This would be the case if the eigenvalue associated with B-1 were positive, then the equilibrium shift A-2 to B-1 would cause an immediate instability. This consequence is more likely to occur at high loading levels. A more interesting case involves B-1 and B-2 together. Under certain conditions, a bifurcation point may materialize in the vicinity of B-1 due to the alteration of the dynamical system structure by the limiting constraint. The consequence of this is that two equilibria, one stable and one unstable, may now lie in close proximity in state space. This would be the case if the equilibria B-2 were to appear in close proximity to B-1. As the power system is subjected to small, dynamic changes, the physical system state may tend toward either of the two equilibria along a trajectory on the unstable manifold. If the equilibrium approached in stable, then the system response will be stable, albeit with a reduced margin of stability. If, however, the trajectory tends toward the unstable equilibrium, the system response will be unstable, and without corrective actions, a voltage collapse may occur.

The correlation between equilibria is illustrated in Fig. 1. The curved function in this figure corresponds to the manifold defined by the relationship between x_1 and y for a constant input u [(10) with $x_1 = 0$ and (12)]. This manifold will change as u varies. The linear functions represent the constraint imposed by the equation for x_2 . The line #1 corresponds to (11) with $\dot{x}_2 = 0$ and line #2 corresponds to (13). The intersection of line #1 with the manifold gives the equilibria A-1 and A-2 of the unlimited system. The intersection of line #2 with the manifold gives the equilibria B-1 and B-2 of the limited system, where the points A-2 and B-1 are identical operating points, but with different stability margins.

Consider the case where the parameters $k_1 - k_7$ are such that B-1 is stable and B-2 is unstable (Normally, k_1 would not be negative, but due to the simplification of the model, it is illustrative to consider this possibility). As the load increases or decreases, the points B-1 and B-2 may tend toward or away from each other. At some loading level, these two equilibria, one stable and one unstable, may coalesce into a single equilibrium. If the two equilibria annihilate one another such that no equilibria exist for increased loading levels, a saddle-node bifurcation has occurred. This type of bifurcation has been shown to be a frequent cause of voltage collapse [8], [9]. As the power system is subjected to dynamic changes, such as changes in load, the system state will move along a trajectory on the system manifold until one of the equilibria is reached. If this equilibrium is the stable equilibrium, the system response will be stable. If the trajectory tends toward the unstable equilibrium, the system response will be

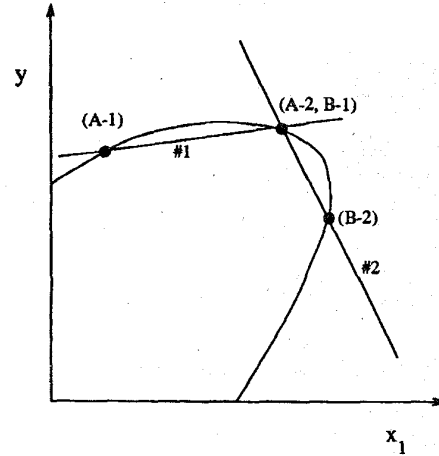


Fig. 1. Correlation between operating points A-1, A-2, B-1, and B-2.

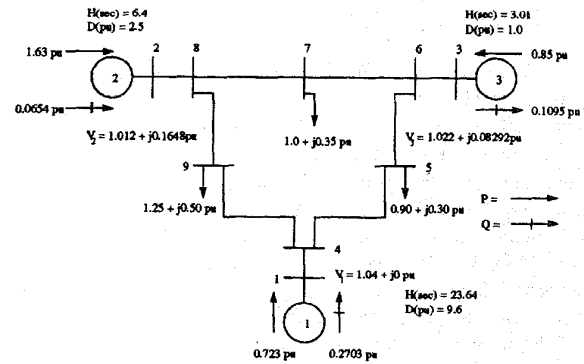


Fig. 2. WSCC 9 bus, 3 generator system.

unstable, and without corrective actions, the system may experience a voltage collapse. Either outcome is possible, but as discussed in the next section, the unstable equilibrium tends to be the more likely of outcomes, due to the dynamic responses of the other AVR's in the system. This behavior is illustrated in greater detail in the following section with a power system example.

IV. POWER SYSTEM EXAMPLE

In this example, the well-known 9-bus, 3-generator WSCC system [10] (Fig. 2) is subjected to a system wide loading increase from the loads stated in Fig. 2 to $S_5 = 1.35 + j0.45$, $S_7 = 1.50 + j0.66$, and $S_9 = 2.19 + j0.87$. The generator parameters are as given in [10] and the excitation system data is summarized in Table III.

As the load increases, the voltage regulator outputs of all generators will increase in order to maintain the terminal voltages at the specified level and to increase the amount of reactive power generated. The voltage regulator output of generator #2 reaches its maximum value shortly before the maximum loading level is reached. The stable and unstable equilibria of the limited system at the final loading level are given in Table IV, as well as the eigenvalues for the final loading equilibria. Note that the limited system equilibria are very close, and are virtually indistinguishable. In fact, the eigenvalues of the stable and unstable limited system equilibria are more similar than are the eigenvalues of the identical equilibrium points (A-2 and B-1) evaluated for both the unlimited and limited system configuration. The point A-2 has one more eigenvalue associated with it due to the

TABLE III
WSCC SYSTEM EXCITATION DATA

State	Gen 1	Gen 2	Gen 3
E_{fd}^{max}	0.910	0.740	0.850
$0.75 E_{fd}^{max}$	0.670	0.530	0.620
V_R^{max}	4.600	4.600	7.000
V_{ref}	1.080	1.092	1.075
T_E	0.785	0.730	1.400
K_E	1.000	1.000	1.000
T_A	0.020	0.020	0.020
K_A	40.000	40.000	40.000
T_F	1.000	1.000	1.000
K_F	0.030	0.030	0.030

TABLE IV
EQUILIBRIA OF THE WSCC SYSTEM

	A-2/B-1	B-2	Eig A-2	Eig B-1	Eig B-2
ω_1	377.00	377.00	-0.586	-0.031	0.061
δ_1	0.1113	0.1095	$\pm j 0.467$	(-0.647	(-0.685
E'_{f1}	1.1105	1.1226	(-0.800	$\pm j 0.682$	$\pm j 0.677$
E_{d1}	0.0426	0.0419	$\pm j 0.704$	-1.013	-1.013
E'_{fd1}	1.2268	1.2568	-1.181	-1.320	-1.267
V_{R1}	1.8390	1.8944	-2.026	-2.024	-2.038
R_{F1}	0.0368	0.0377	(-0.658	(-0.780	(-0.567
P_{G1}	1.3738	1.3738	$\pm j 2.561$	$\pm j 1.876$	$\pm j 1.966$
Q_{G1}	1.2678	1.4931	(-3.125	(-2.968	(-2.872
ω_2	377.00	377.00	$\pm j 0.295$	$\pm j 0.301$	$\pm j 0.297$
δ_2	1.1369	1.2533	(-4.515	-3.737	-3.737
E'_{f2}	0.8810	0.7980	$\pm j 0.577$	-4.509	-4.661
E_{d2}	0.6605	0.6614	(-5.209	(-5.003	(-5.024
E'_{fd2}	2.6437	2.6437	$\pm j 2.921$	$\pm j 3.036$	$\pm j 2.727$
V_{R2}	0.0793	0.0793	-8.648	-8.430	-8.098
R_{F2}	4.6000	4.6000	-26.251	-26.263	-26.647
P_{G2}	2.2829	2.2829	-48.231	-48.434	-48.436
Q_{G2}	0.7030	0.5384	-48.442	-49.130	-49.135
ω_3	377.00	377.00	-49.132	-60.343	-60.401
δ_3	1.0912	1.0339	-60.345		
E'_{f3}	0.8394	0.9005			
E_{d3}	0.6759	0.6362			
E'_{fd3}	2.4584	2.6115			
V_{R3}	3.8014	4.1129			
R_{F3}	0.0737	0.0783			
P_{G3}	1.4944	1.4944			
Q_{G3}	0.3342	0.5081			
V_1	1.0337	1.0323			
V_2	0.9792	0.9235			
V_3	0.9798	0.9720			
V_4	0.9661	0.9522			
V_5	0.9260	0.9089			
V_6	0.9640	0.9457			
V_7	0.9196	0.8834			
V_8	0.9456	0.9004			
V_9	0.8813	0.8521			

fact that V_{R2} is a state variable, whereas in B-1 and B-2 it is an algebraic variable.

As noted previously, as the system approaches the final loading level, the system may tend toward either of the two equilibria, if they lie near each other along a trajectory on the system manifold. If the effect of the system structure change is to place the operating condition near the unstable equilibrium, the system trajectory may pass by the unstable equilibrium before reaching a stable equilibrium, leading to unstable behavior. As the loading on the system increases, the terminal voltages will initially decrease until the AVR's act to raise the voltages to the voltage set point. As noted previously, the unstable equilibrium is identified by the lower voltages associated with it. The result of the "healthy" AVR's is that the action of raising the system voltages forces the system to pass by the unstable equilibrium before the region of attraction of the stable equilibrium

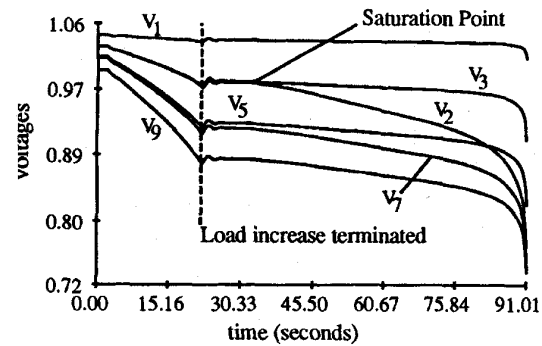


Fig. 3. Dynamic response of the WSCC system when the AVR limit is reached.

is reached. This may cause the system to tend toward the unstable equilibrium, and ultimately, toward voltage collapse. This scenario is illustrated by the dynamic response of the WSCC system voltages in Fig. 3.

The upper limit of V_R for generator #2 is reached shortly after the maximum loading level is reached. The field voltage E_{fd} saturates and reaches its maximum level about 10 seconds later. Prior to this point, the system appears to have attained an equilibrium as the voltages level off and are maintained at a constant level. However, this is an unstable equilibrium and the small dynamic changes in the system perturb the system away from this operating point. In the constrained system, it is no longer possible to hold the terminal voltage of generator #2 to a steady and stable level, since the controlling effects of the exciter have been disabled. As V_2 decreases, there is no longer a closed loop control to maintain the system integrity and the system voltages eventually collapse.

One means of averting this instability is to move the limited generator back into the region of unconstrained operation. One effective control action is to increase the voltage reference setpoint at the generator which has the largest reactive power reserve margin. This strategy has been tested in this example by increasing the voltage reference setpoint of generator #1 by 2%. This accomplishes the goal of reactivating the voltage regulator of generator #2. It does so by introducing more reactive power into the system. The strain on the constrained generator is then relieved, and the exciter is able to return to its normal operating mode. If this corrective action is taken within approximately 50 seconds after the field voltage saturates, the system will recover to a stable operating point. Resetting the reference voltage setpoint is becoming well accepted as a corrective method in voltage collapse situations, with this action becoming an automated function within the control center [11].

V. CONCLUSION

It is often the objective of many control strategies to move the power system operating point away from regions where a bifurcation may occur. Many proposed stability margin indexes attempt to give a measure of the distance from the current operating point of the system to the nearest bifurcation point. In the unconstrained system, the two equilibria are usually sufficiently far apart such that bifurcation is not an immediate concern. However, the change in structure of the differential-algebraic system may suddenly cause a bifurcation point to materialize in the vicinity of the operating point. Although the operating point is unchanged, the stability or stability margin of this point may have changed considerably. Therefore, stability margins or indexes which do not account for the possibility of maximum excitation limits (or reactive power limits) may give false results

which cause the system to appear more stable than it actually is. Due to the discontinuous nature of the instability, any productive corrective action should endeavor to move the system back into an unlimited region of operation. The most promising corrective action scheme for this would be a coordinated control of the AVR reference voltage settings.

REFERENCES

- [1] P. Kundur, *Power System Stability and Control*. New York: McGraw-Hill, 1994.
- [2] K. Walve, "Modeling of power system components at severe disturbances," in *Int. Conf. Large High Voltage Electric Systems*, Paris, France, Aug. 27–Sept. 4, 1986.
- [3] J. H. Chow and A. Gebreselassie, "Dynamic voltage stability analysis of a single machine constant power load system," in *Proc. 29th Conf. Decision and Control*, Honolulu, HI, Dec. 1990.
- [4] C. Rajagopalan *et al.*, "Dynamic aspects of voltage/power characteristics," *IEEE Trans. Power Syst.*, vol. 7, pp. 990–1000, Aug. 1992.
- [5] R. Koessler and J. W. Feltes, "Time-domain simulation investigates voltage collapse," *IEEE Computer Applications in Power*, vol. 6, pp. 18–22, Oct. 1993.
- [6] I. Dobson and L. Lu, "Voltage collapse precipitated by the immediate change in stability when generator reactive power limits are encountered," *IEEE Trans. Circuits Systems: I*, vol. 39, pp. 762–766, Sept. 1992.
- [7] P. W. Sauer and M. A. Pai, *Modeling and Simulation of Multimachine Power System Dynamics Control and Dynamic Systems*, C. Leondes, Ed., vol. 43, 1991.
- [8] C. A. Canizares *et al.*, "Point of collapse methods applied to AC/DC power systems," *IEEE Trans. Power Syst.*, vol. 7, pp. 673–683, May 1992.
- [9] H.-D. Chiang and R. Jean-Jumeau, "Toward a practical performance index for predicting voltage collapse in electric power systems," *IEEE Trans. Power Syst.*, vol. 10, May 1995.
- [10] P. M. Anderson and A. A. Fouad, *Power System Control and Stability*. New York: IEEE Press, 1994.
- [11] J.-P. Paul, J. Y. Leost, and J. M. Tesserion, "Survey of the secondary voltage control in France: Present realization and investigations," *IEEE Trans. Power Systems*, vol. 2, pp. 505–511, May 1987.